NeuroImage: Clinical 3 (2013) 242–248

Contents lists available at ScienceDirect

NeuroImage: Clinical

journal homepage: www.elsevier.com/locate/ynicl

# Periventricular [$^{11}$C]flumazenil binding for predicting postoperative outcome in individual patients with temporal lobe epilepsy and hippocampal sclerosis☆

Josiane Yankam Njiwa [a], Sandrine Bouvard [b,c], Hélène Catenoix [c,d], François Mauguiere [c,d,e], Philippe Ryvlin [c,d,e], Alexander Hammers [a,*]

[a] Neurodis Foundation, Lyon, France
[b] CERMEP-Imagerie du vivant, Lyon, France
[c] Centre de Recherche en Neurosciences de Lyon, France
[d] Service de Neurologie Fonctionnelle et d'Epileptologie, Hôpital Neurologique Pierre Wertheimer, Hospices Civils de Lyon, France
[e] Université de Lyon, Université Claude Bernard, Lyon, France

ARTICLE INFO

*Article history:*
Received 6 May 2013
Received in revised form 5 July 2013
Accepted 25 July 2013
Available online xxxx

*Keywords:*
Mesial temporal lobe epilepsy
Hippocampal sclerosis
Outcome
Periventricular increases
White matter
[$^{11}$C]Flumazenil-PET

ABSTRACT

A third of patients with intractable temporal lobe epilepsy and hippocampal sclerosis (HS) are not seizure free (NSF) after surgery. Increased periventricular [$^{11}$C]flumazenil (FMZ) binding, reflecting heterotopic neuron concentration, has been described as one predictor of NSF outcome at the group level. We aimed to replicate this finding in an independent larger cohort and investigated whether NSF outcome can be predicted in individuals.

Preoperative [$^{11}$C]FMZ summed radioactivity images were available for 16 patients with HS and 41 controls. Images were analyzed using SPM8, explicitly including the white matter, and correction for global radioactivity via group-specific ANCOVA. Periventricular increases were assessed with a mask and different cutoffs for distinguishing NSF and seizure free (SF) patients.

NSF patients had increased [$^{11}$C]FMZ binding around the posterior horn of the ventricles ipsilaterally ($z = 2.53$) and contralaterally ($z = 4.44$) to the seizure focus compared with SF patients. Compared with controls, SF patients had fewer periventricular increases (two clusters, total volume 0.87 cm$^3$, $z_{max} = 3.8$) than NSF patients (two ipsilateral and three contralateral clusters, 6.15 cm$^3$, $z_{max} = 4.8$). In individuals and at optimized cutoffs, five (63%) of eight NSF patients and one (13%) of eight SF patients showed periventricular increases compared with controls (accuracy 75%). Only one (2%) of the 41 controls had increases at the same cutoff.

The association between periventricular [$^{11}$C]FMZ increases and NSF outcome after temporal lobe resection for HS has been confirmed in an independent cohort on simple summed activity images. [$^{11}$C]FMZ-PET may be useful for individual preoperative counseling with clinically relevant accuracy.



## 1. Introduction

Surgical resection of the epileptogenic region is an effective therapy for individuals with medically refractory temporal lobe epilepsy, leading to seizure freedom in about two thirds of patients (Foldvary et al., 2000; Spencer and Huh, 2008; Sperling et al., 1996; Wiebe et al., 2001).

However, this means that around a third of patients with epilepsy and hippocampal sclerosis (HS) undergoing surgery ails to become seizure free. Identification of reliable predictors of suboptimal outcome would be useful for patient management and counseling.

Patients with discrete abnormalities (i.e. lesions or HS) on preoperative MRI have a significantly higher probability of seizure freedom than patients without obvious abnormality (McIntosh et al., 2004). A seizure free outcome is also more likely if the focal lesions visible on MRI are concordant with interictal and ictal EEG and electrocorticography patterns (Yang et al., 2011). Typical patterns of HS include damage in particular to the hippocampal subfields (Lorente de Nó, 1934) CA1 and CA3 (Sommer, 1880) or all subfields (Blumcke et al., 2007).

There is evidence to suggest that atypical histological HS patterns, e.g. damage restricted to the hilar region, may be predictive of poorer outcome (Blumcke et al., 2007; de Lanerolle et al., 2003; Sagar and Oxbury, 1987), including when HS patterns are analyzed quantitatively (Thom et al., 2010).

Other potential biomarkers to predict postoperative NSF outcome postoperatively include higher age at surgery and longer duration of the epilepsy and indicators of early spread of seizures, i.e. presence of hand dystonic posturing and presence of secondarily generalized



* Corresponding author at: Neurodis Foundation, c/o CERMEP-Imagerie du vivant, 59 boulevard Pinel, 69677 Bron, France. Tel.: +33 4 72 68 86 34.
*E-mail address:* alexander.hammers@fondation-neurodis.org (A. Hammers).

2213-1582/$ – see front matter © 2013 The Authors. Published by Elsevier Inc. All rights reserved.
http://dx.doi.org/10.1016/j.nicl.2013.07.008

tonic–clonic seizures. Models constructed based on these variables were at best able to predict seizure status after 24 months with 73% accuracy in a series of 135 patients (Aull-Watschinger et al., 2008). In addition, findings on predictors of NSF outcome are inconsistent (Aull-Watschinger et al., 2008; Hardy et al., 2003; Janszky et al., 2005).

[$^{11}$C]Flumazenil (FMZ) binds to the benzodiazepine sites of $GABA_A$ receptors. Cortical decreases of [$^{11}$C]FMZ binding are associated with epileptogenic foci (Hammers, 2004; Juhász, 2012).

In a series of papers examining white matter (WM) [$^{11}$C]FMZ volume-of-distribution ($V_T$) by voxel-based analysis (statistical parametric mapping, SPM), we have shown the following: 1) WM [$^{11}$C]FMZ $V_T$ correlated strongly with the histologically determined number of heterotopic neurons in the WM (Hammers et al., 2001, 2002), 2) WM [$^{11}$C]FMZ $V_T$ was increased in the temporal lobe in 11/18 individual patients with TLE and normal MRI (Hammers et al., 2002), 3) WM [$^{11}$C]FMZ $V_T$ was increased in periventricular regions in 7/44 patients with extratemporal epilepsy (Hammers et al., 2003b), and 4) periventricular [$^{11}$C]FMZ $V_T$ increases detected by PET in MRI-negative patients appeared identically to such increases due to MRI visible periventricular heterotopia (Hammers et al., 2003b).

Finally, at the group level, increased preoperative periventricular WM [$^{11}$C]FMZ $V_T$ was associated with a postoperative outcome of incomplete seizure freedom after temporal lobe resection for HS (Hammers et al., 2005).

The present study first replicates this association in a new independent cohort of patients with pathologically proven HS, and then extends the work to enable refinement of the post-operative prognosis for individual patients, based on their preoperative [$^{11}$C]FMZ-PET. Instead of [$^{11}$C]FMZ-$V_T$ images, methodologically less demanding summed radioactivity images were used in this study.

## 2. Material and methods

### 2.1. Participants

We retrospectively identified all patients fulfilling the following criteria:

1) Suffering from mesial TLE,
2) HS diagnosed on MRI (confirmed by histopathology for most of the patients),
3) Temporal lobe surgery with a postsurgical follow-up for at least twelve months,
4) Availability of preoperative [$^{11}$C]FMZ PET on the Siemens/CTI HR + PET camera installed at the CERMEP imaging center.

Some of these patients (patients #2, #4, #7, #10, #12, #15, #16) have already been investigated for other questions in other studies (Bouvard et al., 2005; Ryvlin et al., 1998).

The presurgical investigation of candidates for surgery included obtaining each patient's medical history, physical examination, long-term video electroencephalography (VEEG), and, if required, stereotaxic EEG (SEEG). Sixteen patients (four men and twelve women) fulfilled the criteria. Nine had left-sided HS and six right-sided HS, diagnosed on MRI by experienced radiologists and neurologists. All patients had standard anterior temporal lobectomies by the same neurosurgeon; in patient #10, SEEG had shown some seizures to originate in the inferior insula, and she underwent an additional inferior insulectomy (Malak et al., 2009). Postoperative follow-up was 69 ± 33 months (range 23–119). Outcome was assessed according to Engel's classification (Engel 2006) by two epileptologists blinded to the imaging results (FM, PR). Eight patients (50%) were entirely seizure free (Engel class IA) and eight were not (Engel class not IA either continuously or at some stage during follow-up, at least four months after surgery) (Takahashi et al., 2012). The mean age at scan was 34 ± 9 years (range 24–48), the mean age at seizure onset was 7 ± 8 years (range: 1–33) and the mean duration of epilepsy was 25 ± 9 years (range: 12–42). All patients were diagnosed based on history, seizure semiology, MRI, and long-term VEEG. Twelve of the sixteen patients had also undergone SEEG, to exclude one of the following: neocortical onset (n = 4); bilateral onset (n = 4); perisylvian onset (n = 4). Table 1 shows the clinical characteristics of the patients. Potential differences between SF and NSF patients in age at seizure onset, duration of epilepsy and age at operation were assessed with Mann–Whitney U tests.

HS was confirmed on histology in 14/16 cases. As the surgical technique utilized did not use "en bloc" resections, the material available was variable, and in two patients (#13 and #16) no firm conclusions regarding the hippocampus could be drawn. Histology also showed additional microdysgenesis (#3), discrete dysgenesis of the amygdala (#4)/cystic lesion of the amygdala interpreted as ependymal canal heterotopia (#12), small heterotopia of the temporal pole (#10, #16), and additional chronic ischemic lesions (#15).

[$^{11}$C]FMZ PET scans of forty-one control subjects (20 men and 21 women) with a mean age of 35 ± 10 years were available, obtained on the same camera with the same protocol. They all had normal MRI and were not treated with any regular medication.

Written informed consent had been signed by control subjects at the time of PET scanning in agreement with the French legislation and after approval by the local Ethics committee.

### 2.2. PET data acquisition

FMZ (RO15-1788) was radiolabeled with $^{11}$C using methylation (Maziere et al., 1984). PET scans were acquired using an Exact ECAT HR+ scanner (Siemens, Erlangen, Germany) in the high sensitivity three-dimensional mode with a spatial resolution of about 5 mm full with half maximum (FWHM) measured with $^{18}$F according to the NEMA protocol (Brix et al., 1997). For the purpose of attenuation correction, a $^{68}$Ge transmission scan was acquired.

[$^{11}$C]FMZ (2.775 MBq/kg) and unlabelled FMZ (0.01 mg/kg) were simultaneously injected (Delforge et al., 1995).

Starting at injection, dynamic three-dimensional emission images were collected as twelve consecutive temporal frames over 55 min and reconstructed as sixty-three contiguous slices with 2.42 mm slice thickness and a voxel size of either 1.69 × 1.69 × 2.43 mm (data sets acquired until 2000) or 1.72 × 1.72 × 2.43 mm (data sets acquired from 2000), corrected for attenuation and scatter. The partial saturation method (Delforge et al., 1995) is normally used to obtain parametric $B_{max}$ images. However, it has recently been shown that summed [$^{11}$C]FMZ radioactivity images obtained from data acquired using this protocol over the last five frames (20–55 min post-injection) are more reliable, with regional intraclass correlation coefficients approaching 0.8 on average (Bouvard et al., 2012).

### 2.3. PET data analysis

[$^{11}$C]FMZ summed radioactivity images were analyzed using statistical parametric mapping (SPM8; Wellcome Department of Imaging Neuroscience, UCL, London, UK; http://www.fil.ion.ucl.ac.uk/spm).

#### 2.3.1. Spatial preprocessing and quality control

The images of the seven right HS patients (3/8 SF and 4/8 NSF) were right–left reversed prior to normalization to lateralize the epileptologic side to the left for all patients for group analyses.

As 7/16 patient data sets were right–left reversed, the same percentage of control data sets was reversed. The controls to be flipped were chosen at random (www.random.org). There were no substantial differences in analysis results (activated clusters, z scores etc.) compared to analyses with unflipped controls.

An in-house [$^{11}$C]FMZ template in the standard Montreal Neurological Institute (MNI) space based on thirty eight healthy subjects scanned on the same scanner was available. Because a proportion of the raw

**Table 1**
Clinical data for 16 patients with refractory mTLE and HS. CBZ = Carbamazepine, CLB = Clobazam, LEV = Levetiracetam, LTG = Lamotrigine, PB = Phenobarbital, PHT = Phenytoin, PRG = Pregabaline, TPM = Topiramate, VPA = Valproic Acid. M = male, f = female, HS = hippocampal sclerosis, CE = cluster extent, H = Hippocampus. Postoperative outcomes for non-seizure free patients are given in the footnotes, including times when the outcome class changed.

| Patient | Age/sex | Onset/duration of epilepsy (years) | MRI: HS | Follow-up (months) | Antiseizure medication at operation *: reduced **: stopped (medication restarted) | Outcome (Engel class) | [$^{11}$C]FMZ-PET increases in periventricular areas (TH = 0.01, z > 3.2, p < 0.46) | Additional information |
|---|---|---|---|---|---|---|---|---|
| #1 | 24/f | 6/18 | L | 57 | LEV, LTG* | IA | None | Additional L temporo-occipital dysplasia on MRI |
| #2 | 22/f | 2/20 | L | 58 | CBZ, TPM, CLB** | IA | None | Additional amygdala atrophy on MRI |
| #3 | 27/m | 4/23 | L | 35 | CBZ, VPA, CLB** | IA | None | |
| #4 | 36/f | 3/33 | L | 98 | CBZ, LTG, TPM** | IA | None | Additional L temporal pole signal abnormalities on MRI; discrete dysgenesis of L amygdala on histology |
| #5 | 46/f | 12/34 | L | 71 | PB, PRG, LEV* | IA | None | |
| #6 | 26/f | 5/21 | R | 112 | CBZ, CLB, PB*, | IA | R lat of ventricle z = 4.18 (42–36 8), CE = 2.2 cm$^3$ | Additional R temporal pole signal abnormalities on MRI |
| #7 | 48/f | 6/42 | R | 81 | CBZ, CLB** | IA | None | |
| #8 | 30/f | 5/25 | R | 24 | CBZ, TPM, CLB, LEV** | IA | None | |
| #9 | 46/f | 33/13 | R | 23 | PHT, LEV, PB** | IB[a] | None | |
| #10 | 36/f | 3/33 | R | 116 | CBZ, PB, CLB | IVB[b] | None | Seizure onset right temporal and right insular on SEEG |
| #11 | 29/f | 4/25 | R | 44 | CBZ, CLB** | IIA[c] | None | Small symmetric hippocampi and temporal pole signal abnormalities on MRI; FDG PET: R mesial temporal hypometabolism; SEEG: unilateral R onset |
| #12 | 32/m | 5/27 | L | 119 | PB, CLB** (LEV, CLB) | IIA[d] | Widespread WM increases (CE 15.3 cm$^3$) with the maximum L ant of frontal horn z = 6.02 (−20 34 −4), but extending bilaterally with other maxima anterior to both frontal horns and postero-lateral of right lateral ventricle Lateral of posterocentral portion of L lateral ventricle z = 4.62 (−34 −44 14), CE = 3.7 cm$^3$ Lateral of posterior portion of R lateral ventricle z = 4.12 (30 −60 12), CE = 6.5 cm$^3$ | |
| #13 | 32/f | 11/21 | L | 89 | CLB, CBZ** (CBZ, PB) | IID[e] | Lateral of anterocentral portion of R frontal horn z = 3.27 (24 12 16), CE = 4.0 cm$^3$ L anterior of frontal horn z = 3.82 (−18 36 −4), CE = 5.0 cm$^3$ | |
| #14 | 22/m | 9/13 | L | 72 | CBZ, TPM, PB, CLB** | ID[f] | Lateral of posterocentral portion of L lateral ventricle z = 4.51 (−34 −48 16), CE = 1.7 cm$^3$ L anterior of frontal horn z = 3.96 (−14 38 −2), CE = 1.7 cm$^3$ | |
| #15 | 39/m | 1/38 | L | 67 | TPM, PB* | IIA[g] | Lateral and inferior of L ventricle where temporal and occipital horns originate n z = 4.01 (−30 −52 4), CE = 3.0 cm$^3$ Lateral and inferior of R ventricle z = 3.29 (10 6 4), CE = 2.4 cm$^3$ | |
| #16 | 41/f | 3/38 | R | 78 | LTG, CBZ, PB* | IC[h] | Lateral and inferior of R ventricle where temporal and occipital horns originate z = 3.22 (32 −48 4), CE = 1.8 cm$^3$ | Additional moderate gliosis R temporal pole on MRI + L ventricular enlargement |

[a] IB at 5 months and IA at 17 months.
[b] Never seizure free.
[c] IB at 5, 10, and 23 months, ID at 16 months and IA at 29 and 35 months.
[d] IA until 110 months.
[e] IA at 19 months and IID at 31 months.
[f] ID at 60 months.
[g] IIA at 67 months.
[h] IC at 12 and 21 months.

images was left–right reversed, this template was symmetrized for group analyses as described earlier (Didelot et al., 2010).

All images of the study were spatially normalized (Ashburner and Friston, 1999) to this symmetric [$^{11}$C]FMZ template. The normalized images were smoothed using an isotropic Gaussian kernel of 10 mm FWHM.

For individual analyses, the original, asymmetric [$^{11}$C]FMZ template was used, i.e. individual images were not flipped. The preprocessing was otherwise identical.

Differences in global values influence the global scaling procedure in SPM and could hence in principle explain differences in low-binding areas like the periventricular white matter. The global mean was calculated via the spm functions spm_global.m and spm_global.c in a two-step procedure. After the computation of the mean over all voxels, the mean of values above 1/8 of the overall mean is calculated. Global means were compared between SF patients, NSF patients and controls using two-tailed Student's t-tests.

#### 2.3.2. SPM analyses

We used a combination of low-threshold relative masking and an explicit mask to include the whole white matter (WM) in the SPM8 analysis, as described earlier (Hammers et al., 2003b). The periventricular region was objectively assessed with a mask constructed with basic SPM8 functions as follows: The ventricles were isolated from a maximum probability human brain atlas in MNI space (Hammers et al., 2003a). This region was then dilated by 10 mm, to include ~10 mm tissue around the ventricular system (Hammers et al., 2003a). The resulting boundaries were regularized by smoothing the mask with a $10 \times 10 \times 10$ mm$^3$ (FWHM) isotropic Gaussian kernel and thresholding at 0.25.

The statistical model included correction for global radioactivity via a group-specific analysis of covariance (ANCOVA).

Group analyses followed by individual analyses were performed to assess periventricular increases within the mask described above. At the group level, the aims were to replicate our earlier finding of differences between patients with suboptimal outcome and SF patients; and to compare both of those groups with the control group. At the individual level, each control was compared against the remaining forty controls and each patient against all forty one controls, in order to investigate whether periventricular increases can be used at the individual level to predict postoperative outcome.

The linear contrasts used to test focal effects resulted in sets of voxel values for each contrast which constituted parametric maps of t statistics. The maps were thresholded at $p = 0.01$ uncorrected, as in our previous study (Hammers et al., 2005). The unusually lenient initial threshold is justified by the low number of "resolution elements" (corresponding to independent spatial samples) in the periventricular mask ($n = 55$ "resels").

We then investigated different combinations of cluster characteristics in order to best differentiate between SF patients and NSF patients. For the descriptive statistics of the clusters found in the periventricular mask, we searched for optimum discrimination for the two parameters "uncorrected cluster probability" and "z value of peak voxel".

The cluster probability search space was set to 0.00–0.99 in steps of 0.01 for cluster p values. The peak voxel z score search space was any value above 3.5 in steps of 0.5. Within this search space, all combinations were tested for their ability to optimally discriminate SF and NSF patients. In the present sample, the optimal conditions for distinguishing SF and NSF patients were considering clusters in the periventricular mask fulfilling the combined condition of a z score >3.5 for the peak voxel together with a cluster p value ≤0.5.

## 3. Results

### 3.1. Global values

The global values of the summed radioactivity images after spatial normalization did not differ significantly between groups. The mean global values were 2202 ± 216 for SF patients, 2182 ± 303 for NSF patients, and 2409 ± 269 for controls ($p_{min} = 0.09$).

### 3.2. Group analyses

#### 3.2.1. NSF versus seizure-free patients

NSF patients had higher FMZ binding than seizure free patients around the posterior horn of the ventricles ipsilaterally to the seizure focus at threshold $p < 0.01$ (maximum $z = 2.7$) and contralaterally (maximum $z = 4.2$). We thus replicated the findings in our previous study (Hammers et al., 2005). In addition, in the present sample some clusters were located around the anterior horns (see Fig. 1(c)).

There were no significant differences between seizure free and NSF patients for the other potential predictors for postoperative NSF outcome, namely sex, age at seizure onset, age at surgery, and duration of epilepsy. Results for the continuous variables are illustrated in Table 2.

#### 3.2.2. Patient groups against controls

The group of seizure free patients had three ipsilateral clusters of increased periventricular [$^{11}$C]FMZ binding compared with controls (0.9, 0.45 and 0.25 cm$^3$, maximum $z = 3.31$) as illustrated in Fig. 1(b).

In contrast, the group of NSF patients compared with controls had more and larger clusters of increased periventricular [$^{11}$C]FMZ binding, with higher z scores: two ipsilateral clusters (3.0 and 2.9 cm$^3$, maximum $z = 5.25$), and three contralateral clusters (3.8, 2.2 and 0.8 cm$^3$, maximum $z = 4.33$; see Fig. 1(a)).

### 3.3. Individual analyses

Periventricular increases in individual patients occurred in similar regions as in the group analyses. Under the optimal threshold conditions detailed in the Material and methods section, five of eight suboptimal outcome patients (63%) showed periventricular increases for [$^{11}$C]FMZ binding when compared individually against the control group (Table 1). One of the eight seizure free patients (13%) and one of the 41 controls (2%) also showed periventricular [$^{11}$C]FMZ increases.

When considering the presence of periventricular increases as a test indicating NSF outcome, the test had a sensitivity of 63% (i.e. 5/8 NSF patients were correctly identified), a specificity of 88% (i.e. absence of periventricular increases correctly predicted SF outcome in 7/8 patients), a precision of 83% (i.e. the prediction of NSF outcome was correct in 5/6 patients with periventricular increases) and an accuracy of 75% (i.e. results were correct in 12/16 patients overall). Table 3 recapitulates the performance of the test performed on the available data. Fig. 1(d) illustrates areas of increased periventricular [$^{11}$C]FMZ binding in an individual NSF patient (patient #15).

## 4. Discussion

The association between periventricular increases of [$^{11}$C]FMZ radioactivity concentration with NSF outcome after temporal lobe resection for HS has been confirmed at the group level in an independent cohort, using simple summed activity images.

Our previous study used methodologically more demanding fully quantified $V_T$ images which require an arterial input function (Hammers et al., 2005). In another previous study, $V_T$ images were superior to both binding potential ($BP_{ND}$) images obtained with an image-based input function and summed activity images for detecting the epileptogenic abnormality in hippocampal sclerosis (Hammers et al., 2008). An important result of the present investigation is that simple summed radioactivity images, without requirement for a metabolite-corrected arterial plasma input function, are sufficient for the purpose of preoperatively showing periventricular increases in NSF patients after surgery.

Other studies have shown that the complete absence of seizure varies widely with the postoperative time (Aull-Watschinger et al.,

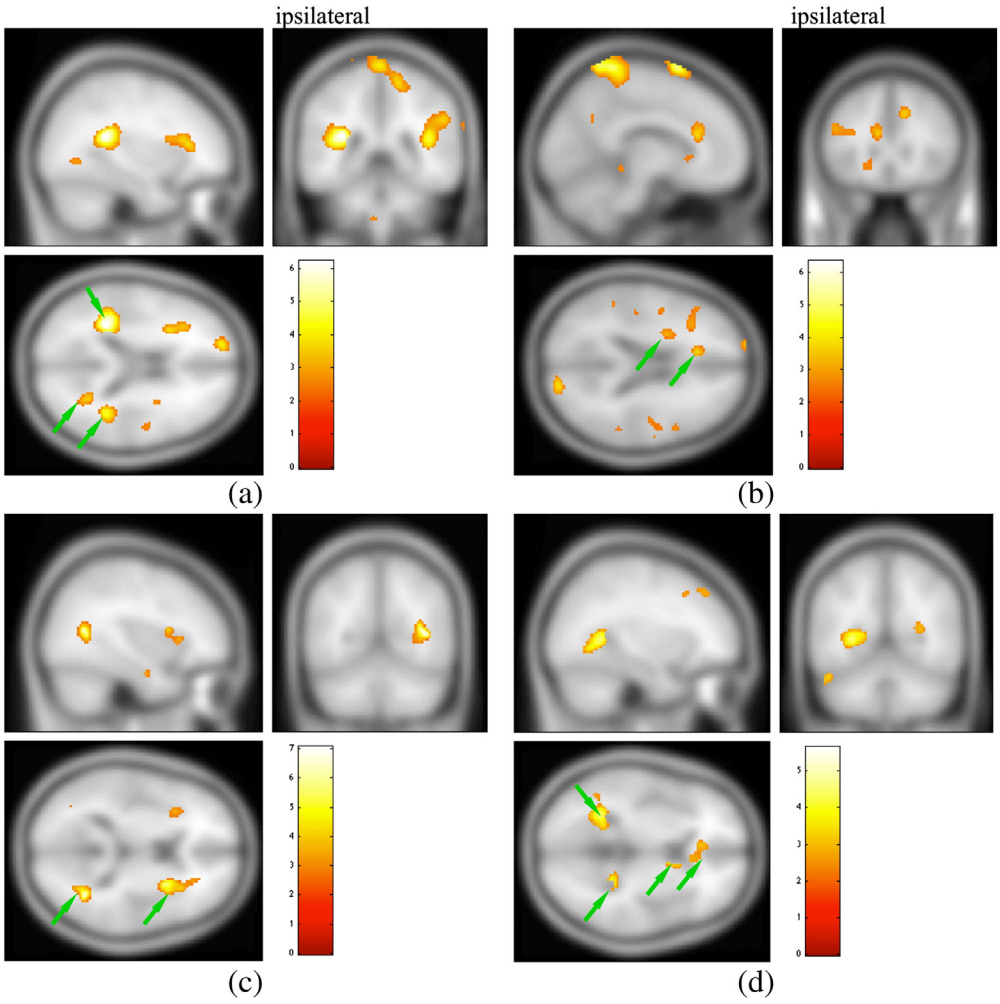


**Fig. 1.** Periventricular increases. Statistical results, visualized at $p < 0.01$, overlaid on the SPM8 T1-weighted template. All results are unmasked and therefore clusters outside of the periventricular mask used for statistical assessment are also shown. Left on the image is ipsilateral to the side of surgery. Clusters with highest z-scores observed within the periventricular mask are highlighted with green arrows. The notation CE stands for cluster extent. Color bar, t scores. (a) Increases in patients with suboptimal outcome (not Engel class IA), compared to controls ($z_{max} = 5.3$ ipsilaterally (CE = 3 $cm^3$) and $z_{max} = 4.3$ contralaterally (CE = 2.2 $cm^3$)). (b) Patients with Engel class IA outcome have far less important periventricular increases compared to controls ($z_{max} = 3.3$, CE = 0.3 $cm^3$). (c) Increases in patients not Engel IA compared to seizure-free patients; contralateral ($z_{max} = 4.2$,m CE = 0.9 $cm^3$) and ipsilateral ($z_{max} = 2.7$, CE = 0.56 $cm^3$). This is the same comparison as in the cohort in Hammers et al. (2005). (d) Periventricular increases in an individual patient with suboptimal outcome, posterior to the ipsilateral lateral ventricle ($z_{max} = 4.0$, CE = 3.0 $cm^3$).

2008; Elsharkawy et al., 2009; Kelemen et al., 2006). For example, in one study of 153 patients with MRI-diagnosed HS sex, seizure frequency before the operation, and unilaterality of interictal EEG discharges were used as variables in a logistic regression equation to predict outcome after surgery (Aull-Watschinger et al., 2008). Complete seizure freedom (Engel class IA) could not be predicted from conventional preoperative variables.

Our hypothesis, based on the prior work cited in the introduction, is that periventricular white matter increases of [$^{11}$C]FMZ binding indicate an increased concentration of heterotopic neurons. These could represent a developmental abnormality, i.e. MRI-invisible subependymal heterotopia (Hammers et al., 2003b), or be secondary to frequent seizures. In either case, there would be dual pathology expected to lead to a stronger tendency for ongoing seizures after removal of the main epileptogenic focus. This would reflect the existence of a more widespread epileptogenic network extending beyond the hippocampus and beyond the limits of temporal lobectomies. Accordingly, we used the strict criterion of non-Engel IA outcome at any time during follow-up, similar to our previous study (Hammers et al., 2005).

Patients selected for [$^{11}$C]FMZ PET had more complex electro-clinical patterns than usual, which explains the rather high proportion of patients having undergone SEEG. Regions often investigated as possible alternative areas of seizure onset include the insula, the posterior temporal neocortex, the temporo–parieto-occipital junction, the supra-sylvian operculum, and the orbito-frontal cortex. In this group, SEEG was often used to confirm mesial temporal onset or exclude an extratemporal

**Table 2**
Evaluation of other potential predictors of NSF = not seizure free epilepsy surgery outcome.

| Predictor (median, [lower; higher quartile]) | SF patients | NSF patients | Mann–Whitney U test |
|---|---|---|---|
| Age at onset (years) | 5 [3.8; 6.0] | 4.5 [3.0; 9.5] | 32.5 ($p = 0.96$) |
| Epilepsy duration (years) | 24 [20.8; 33.3] | 26 [19; 34.3] | 32.5 ($p = 0.96$) |
| Age at operation (years) | 28.5 [25.5; 38.5] | 34 [31.5; 39.5] | 38.5 ($p = 0.51$) |

**Table 3**
Test performance. SF = seizure free, NSF = not seizure free.

| | Clinical outcome | | |
|---|---|---|---|
| Test output | | SF | NSF |
| | SF | 7 | 3 |
| | NSF | 1 | 5 |

seizure onset; the series is surgically homogenous with all patients having undergone standard temporal lobectomies.

SEEG electrodes record from a diameter of at most 10 mm. SEEG electrode locations were determined clinically and did not normally include periventricular areas which are far from the hippocampus (see Fig. 1) and are not included in the resection volume for temporal lobectomies. For these reasons, we cannot determine whether periventricular clusters of increased FMZ binding show interictal epileptiform abnormalities.

In our small sample, sex did not influence the postoperative outcome, consistent with other studies (Burneo et al., 2008; Elsharkawy et al., 2009; Yang et al., 2011). Some studies found an effect of age at surgery and epilepsy duration on postoperative outcome (Janszky et al., 2005), while others did not (Aull-Watschinger et al., 2008; Hardy et al., 2003; Kilpatrick et al., 1999). Again, in our small sample, there was no significant influence of age at seizure onset and longer duration of epilepsy. In this context, it is remarkable that periventricular increases of [$^{11}$C]FMZ binding were once again predictive of NSF outcome, despite the small sample size, similar to the sample size in the earlier paper (Hammers et al., 2005).

We observed that all patients presenting periventricular increases (6/6 patients) were taking GABA-ergic anti-epileptic drugs (AEDs) compared with 6/10 of patients without periventricular increases. We therefore checked the effect of GABA-ergic AEDs on FMZ binding. Global values of patients presenting periventricular increases showed no significant differences compared to patients without signal increases ($p > 0.8$). In addition, unlabeled FMZ was administered to all subjects as described in the Material and methods section, therefore a similar fraction of receptors should have been occupied.

In another study, secondarily generalized seizures and ictal dystonia were associated with a worse two-year outcome (Janszky et al., 2005); in this retrospective study of patients operated 5–15 years ago, we did not have systematic data on these variables in our sample.

As would be expected, the prognostic value of potential predictors depends on the post-operative time interval for which the assessment was made, and there is interdependence of prognostic factors (Janszky et al., 2005; Najm et al., 2013). For example, seizure recurrence within six months of surgery was associated with a poor long-term postoperative outcome (Yang et al., 2011). Among the eight patients with NSF outcome in our study, there were six (75%) who were not in Engel class IA after five years the same number as after 1.5 years. Follow-up was only non-significantly shorter in the SF group ($5.1 \pm 2.7$ years) than in the NSF group ($6.3 \pm 2.7$ years; $p < 0.39$), but it cannot be excluded that even a longer follow-up would change some of the classifications.

While the association of periventricular increases of [$^{11}$C]FMZ binding and suboptimal outcome at the group level is pathophysiologically interesting, it does not aid individual counseling. Here, we investigated whether individualized prognosis and hence better management of candidates for epilepsy surgery were achievable. In contrast to our earlier study (Hammers et al., 2005), five of eight NSF patients and seven of eight seizure free patients could be correctly identified using presence or absence of periventricular increases of [$^{11}$C]FMZ binding as the criterion. The most likely explanation for this improvement is the much larger size of the control group, with 41 controls in the present study compared with 13 in the previous study. The importance of the size of the control group has been noted previously (cf. (Pell et al., 2008; Wilke et al., 2008)).

Parameters were optimized within the cohort, which was too small for splitting into training and testing sets. There is therefore a need to replicate the findings in other, independent cohorts.

Of note, strict application of the inclusion criteria led to the presence in the sample of three patients (#1, 10 and 11; see Table 1) with atypical features, which might by themselves indicate a worse prognosis. Interestingly, two of these (and #11) overlapped with the three of the eight patients with suboptimal outcome who did not show WM periventricular increases. This might explain the imperfect sensitivity of periventricular [$^{11}$C]FMZ binding increases, as they thus had other potential reasons for a suboptimal outcome: Patient #10 had HS but also required a partial right insulectomy following the results of SEEG, indicating a larger seizure onset zone than usual, and patient #11 had bilaterally small hippocampi. In contrast, one patient (patient #6) was free of seizures after 112 months of follow-up despite increases of [$^{11}$C]FMZ binding in periventricular regions, showing their imperfect specificity.

It is also important to mention that, from the clinician's perspective, most patients in the NSF group did in fact have a very meaningful improvement in their seizure frequency. In addition, some of the patients classified as NSF according to our strict criteria had identifiable causes for seizure recurrence, for example due to changes in medication (patient #14, patient #15). The meaning of "NSF" in this context would have to be explained to surgical candidates.

Our study suggests that a simplified analysis method, based on summed [$^{11}$C]FMZ radioactivity images and without the need for an arterial input function, suffices for predicting a higher likelihood of NSF postoperative outcome. Nevertheless, [$^{11}$C]FMZ PET is not widely available. Future work should investigate whether more widely available PET tracers with high contrast between gray and white matter, notably [$^{18}$F]fluorodeoxyglucose (FDG), can serve the same purpose. This may also open the option of correlating SEEG results with periventricular increases, which was impossible in this retrospective study as WM contacts are regularly not sampled.

In summary, the association between periventricular WM increases of [$^{11}$C]FMZ binding with suboptimal outcome after temporal lobe resection for HS has been confirmed in an independent cohort on simple summed radioactivity images. Optimized analysis of individual patient data suggests usefulness of [$^{11}$C]FMZ-PET for individual preoperative counseling with clinically relevant accuracy.

## Disclosure of conflicts of interest

None of the authors has any conflict of interest to disclose.

We confirm that we have read the Journal's position on issues involved in ethical publication and affirm that this report is consistent with those guidelines.

## Acknowledgments

We would like to thank our clinical colleagues who followed up the patients, and the neuroradiologists, nuclear medicine physicians and neuropathologists who obtained additional data.

## References

Ashburner, J., Friston, K.J., 1999. Nonlinear spatial normalization using basis functions. Hum. Brain Mapp. 7, 254–266.
Aull-Watschinger, S., et al., 2008. Outcome predictors for surgical treatment of temporal lobe epilepsy with hippocampal sclerosis. Epilepsia 49, 1308–1316.
Blumcke, I., et al., 2007. A new clinico-pathological classification system for mesial temporal sclerosis. Acta Neuropathol. 113, 235–244.
Bouvard, S., et al., 2005. Seizure-related short-term plasticity of benzodiazepine receptors in partial epilepsy: a [$^{11}$C]flumazenil-PET study. Brain 128, 1330–1343.
Bouvard, S., et al., 2012. Test–retest reliability of [$^{11}$C]flumazenil data acquired using the Delforge partial saturation method. J. Cereb. Blood Flow Metab. 32, S167.
Brix, G., et al., 1997. Performance evaluation of a whole-body PET scanner using the NEMA protocol. National Electrical Manufacturers Association. J. Nucl. Med. 38, 1614–1623.
Burneo, J.G., et al., 2008. Kaplan–Meier analysis on seizure outcome after epilepsy surgery: do gender and race influence it? Seizure 17, 314–319.
de Lanerolle, N.C., et al., 2003. A retrospective analysis of hippocampal pathology in human temporal lobe epilepsy: evidence for distinctive patient subcategories. Epilepsia 44, 677–687.
Delforge, J., et al., 1995. Quantification of benzodiazepine receptors in human brain using PET, [$^{11}$C]flumazenil, and a single-experiment protocol. J. Cereb. Blood Flow Metab. 15, 284–300.
Didelot, A., et al., 2010. Voxel-based analysis of asymmetry index maps increases the specificity of $^{18}$F-MPPF PET abnormalities for localizing the epileptogenic zone in temporal lobe epilepsies. J. Nucl. Med. 51, 1732–1739.
Elsharkawy, A.E., et al., 2009. Long-term outcome after temporal lobe epilepsy surgery in 434 consecutive adult patients. J. Neurosurg. 110, 1135–1146.

Foldvary, N., et al., 2000. Seizure outcome after temporal lobectomy for temporal lobe epilepsy: a Kaplan–Meier survival analysis. Neurology 54, 630–634.
Hammers, A., et al., 2001. Neocortical abnormalities of [$^{11}$C]-flumazenil PET in mesial temporal lobe epilepsy. Neurology 56, 897–906.
Hammers, A., et al., 2002. Abnormalities of grey and white matter [$^{11}$C]flumazenil binding in temporal lobe epilepsy with normal MRI. Brain 125, 2257–2271.
Hammers, A., et al., 2003a. Three-dimensional maximum probability atlas of the human brain, with particular reference to the temporal lobe. Hum. Brain Mapp. 19, 224–247.
Hammers, A., et al., 2003b. Grey and white matter flumazenil binding in neocortical epilepsy with normal MRI. A PET study of 44 patients. Brain 126, 1300–1318.
Hammers, A., 2004. Flumazenil positron emission tomography and other ligands for functional imaging. Neuroimaging Clin. N. Am. 14, 537–551.
Hammers, A., et al., 2005. Periventricular white matter flumazenil binding and postoperative outcome in hippocampal sclerosis. Epilepsia 46, 944–948.
Hammers, A., et al., 2008. [$^{11}$C]Flumazenil PET in temporal lobe epilepsy: do we need an arterial input function or kinetic modeling? J. Cereb. Blood Flow Metab. 28, 207–216.
Hardy, S.G., et al., 2003. Factors predicting outcome of surgery for intractable epilepsy with pathologically verified mesial temporal sclerosis. Epilepsia 44, 565–568.
Janszky, J., et al., 2005. Temporal lobe epilepsy with hippocampal sclerosis: predictors for long-term surgical outcome. Brain 128, 395–404.
Juhász, C., 2012. The impact of positron emission tomography imaging on the clinical management of patients with epilepsy. Expert Rev. Neurother. 12, 719–732.
Kelemen, A., et al., 2006. Predictive factors for the results of surgical treatment in temporal lobe epilepsy. Ideggyogy. Sz. 59, 353–359.
Kilpatrick, C., et al., 1999. Seizure frequency and duration of epilepsy are not risk factors for postoperative seizure outcome in patients with hippocampal sclerosis. Epilepsia 40, 899–903.
Lorente de Nó, R., 1934. Studies on the structure of the cerebral cortex. II. Communication of the study of the ammonic system. J. Psychol. Neurol. 46, 113–177.
Malak, R., et al., 2009. Microsurgery of epileptic foci in the insular region. J. Neurosurg. 110, 1153–1163.
Maziere, M., et al., 1984. Synthesis of ethyl 8-fluoro-5,6-dihydro-5-[$^{11}$C]methyl-6-oxo-4H-imidazo [1,5-a] [1,4]benzodiazepine-3-carboxylate (RO 15.1788-$^{11}$C): a specific radioligand for the in vivo study of central benzodiazepine receptors by positron emission tomography. Int. J. Appl. Radiat. Isot. 35, 973–976.
McIntosh, A.M., et al., 2004. Temporal lobectomy: long-term seizure outcome, late recurrence and risks for seizure recurrence. Brain 127, 2018–2030.
Najm, I., et al., 2013. Temporal patterns and mechanisms of epilepsy surgery failure. Epilepsia 54, 772–782.
Pell, G.S., et al., 2008. Selection of the control group for VBM analysis: influence of covariates, matching and sample size. Neuroimage 41, 1324–1335.
Ryvlin, P., et al., 1998. Clinical utility of flumazenil-PET versus [$^{18}$F]fluorodeoxyglucose-PET and MRI in refractory partial epilepsy. A prospective study in 100 patients. Brain 121 (Pt 11), 2067–2081.
Sagar, H.J., Oxbury, J.M., 1987. Hippocampal neuron loss in temporal lobe epilepsy: correlation with early childhood convulsions. Ann. Neurol. 22, 334–340.
Sommer, W., 1880. Erkrankung des Ammonshorns als ätiologisches Moment der Epilepsie. Arch. Psychiatr. Nervenkr. 10, 631–675.
Spencer, S., Huh, L., 2008. Outcomes of epilepsy surgery in adults and children. Lancet Neurol. 7, 525–537.
Sperling, M.R., et al., 1996. Temporal lobectomy for refractory epilepsy. JAMA 276, 470–475.
Takahashi, M., et al., 2012. Voxel-based comparison of preoperative FDG-PET between mesial temporal lobe epilepsy patients with and without postoperative seizure-free outcomes. Ann. Nucl. Med. 26 (9), 698–706.
Thom, M., et al., 2010. Reliability of patterns of hippocampal sclerosis as predictors of postsurgical outcome. Epilepsia 51, 1801–1808.
Wiebe, S., et al., 2001. A randomized, controlled trial of surgery for temporal-lobe epilepsy. N. Engl. J. Med. 345, 311–318.
Wilke, M., et al., 2008. Template-O-Matic: a toolbox for creating customized pediatric templates. Neuroimage 41, 903–913.
Yang, X.L., et al., 2011. Predictors of outcome in the surgical treatment for epilepsy. Chin. Med. J. (Engl) 124, 4166–4171.